

## Main Injector HRF Measurements for Proton Plan

T. Berenc

7/5/2006

**Introduction:** Before the spring 2006 shutdown a series of measurements was made on the h=588 HRF stations as a part of Proton Plan studies to better understand the present operation, to help identify areas of improvement, and to provide experimental data for confirming calculation estimates. This note does not include all the measurements, rather it summarizes the salient features of solid-state drive power, power amplifier DC current, and cavity detuning that impact some of the upgrade decisions.

### SSD Power During a Mixed-Mode Cycle:

The present slip-stacking and mixed-mode (NuMI plus slip-stacking for pBar production) cycles are closest to the Proton Plan multi-batch slip-stacking scheme and are readily available for studies since they are part of day-to-day operations. The present slip-stacking cycle is used to slip-stack only 2 Booster batches and accelerate them to 120GeV for pBar production. The mixed-mode cycle is also used to slip-stack only 2 Booster batches for pBar production; but it also accelerates another 5 Booster batches which are delivered to NuMI.

An example of a typical station response during a mixed mode cycle is shown in Fig. 1 for a slip-stacking 'OFF' station. Figure 1 has been annotated to show the sequence of events within the cycle.

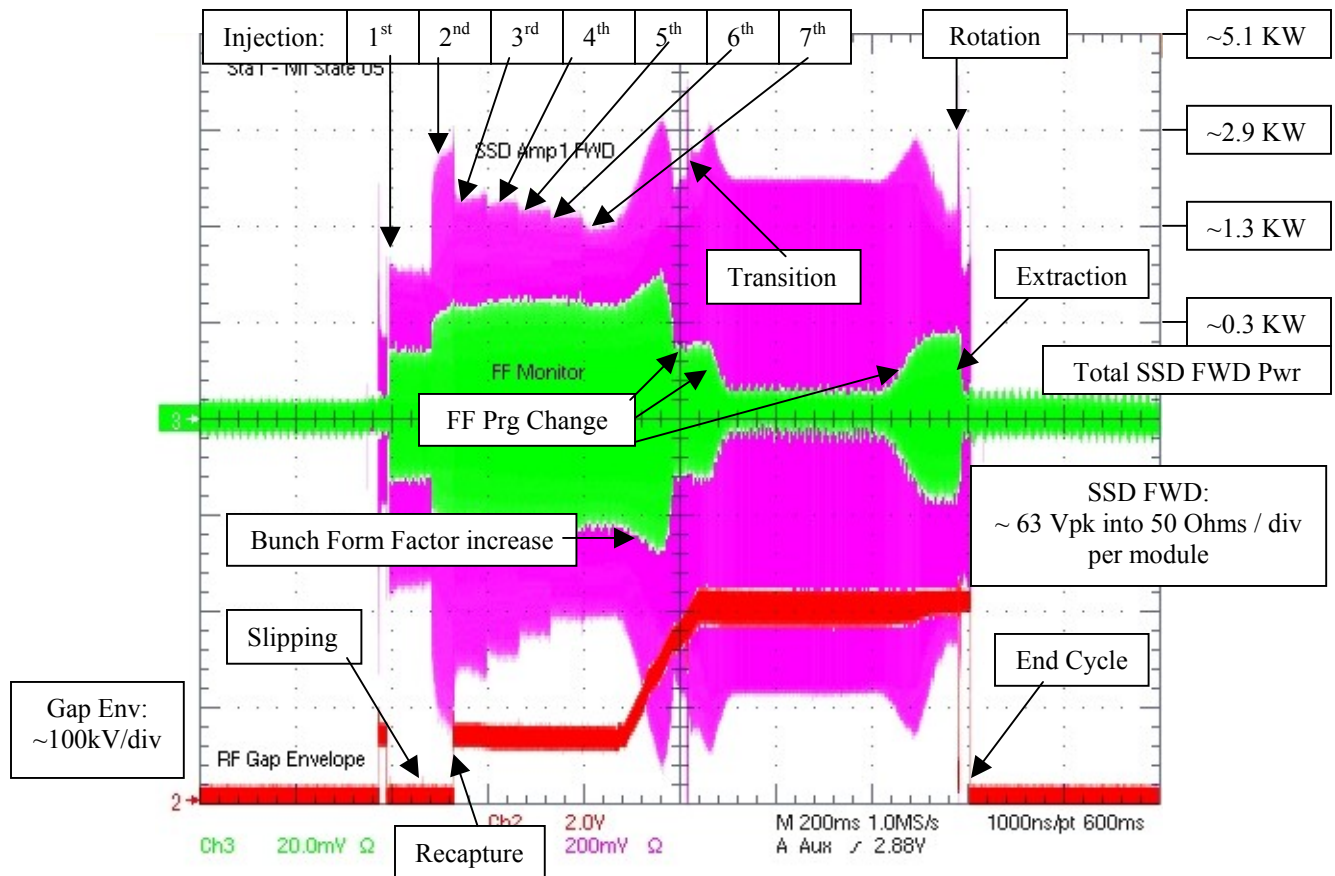


**Figure 1:** Station 1 (Group A 'OFF' station) SSD power during a mixed mode cycle. Single SSD module forward power monitor (magenta), cavity RF gap envelope (red), FF BLC drive signal monitor (green).

In Fig. 1, the SSD forward power monitor is from 1 of 8 1KW SSD amplifier modules. The total SSD forward power from all 8 modules was approximated as 8 times the single module power as annotated on the right of Fig. 1. The FF monitor is in arbitrary units and is meant to show the dynamic programming currently employed and the increase in the bunch form factor. There are 3 distant programming changes in the amount of FF BLC; (1) a decrease right before transition, (2) another decrease after transition, and (3) an increase before bunch rotation. The first increase in the FF after the 2<sup>nd</sup> batch injection is due to the two different batch frequencies beating against each during the slipping and causing the instantaneous FF signal to almost double as the batches slip into each other. The second increase before transition is actually due to the bunch form factor increasing as the bunch length begins to shorten. This bunch form factor increase is predicted in [1].

If the cavity tuning conditions are kept identical to present operations, one could expect the envelope of the SSD forward power to remain as above. With loading more double batches, the peak instantaneous power should remain the same (see the ‘three instantaneous conditions’ technique of Ref [1]). What would change is the average power since the duty factor would increase. Thus from the above, it should be safe to assume that the ‘moving average’ (as denoted in Ref [1]) would have to approach close to 4 - 5kW. The SSD power supplies are rated at 10kW. Assuming that the amplifiers are operating at 50% efficiency, the requirements on the SSD power supplies will be approaching their limits.

To demonstrate that the peak instantaneous power does not go up as more batches are loaded, Figs. 2 and 3 are shown below. These were taken during a multi-batch slip-stacking study. Figure 1 shows the SSD forward power of an ‘OFF’ station after the 1<sup>st</sup> batch injection while Fig. 2 is after the 5<sup>th</sup> batch injection. As the remaining batches are injected and begin slipping, the SSD forward power monitor shows the beating of the two batch frequencies. Also shown is the modulator output current monitors which show the expected increase in average output current.

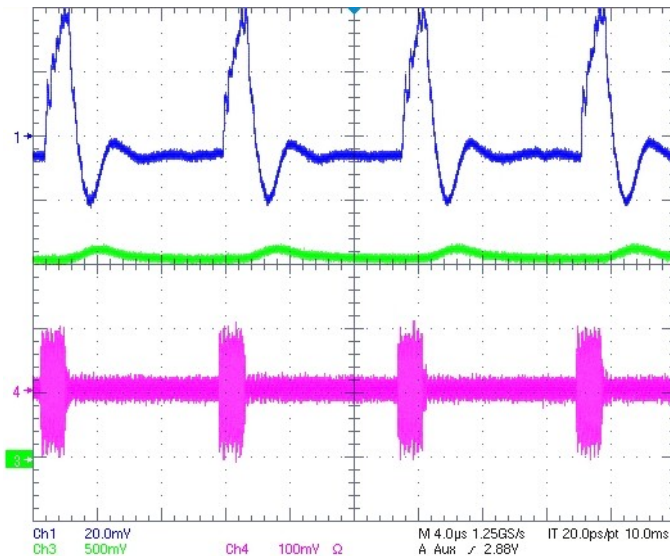


**Figure 2:** SSD forward power monitor 31.6 Vpk into 50 Ohms per module (magenta), modulator output slow current monitor 1A/div (green), modulator output fast current monitor 0.2A/div (blue) on Stal during the 1<sup>st</sup> batch injection of a multi-batch study. Single batch intensity  $\sim 1.7E12$ .

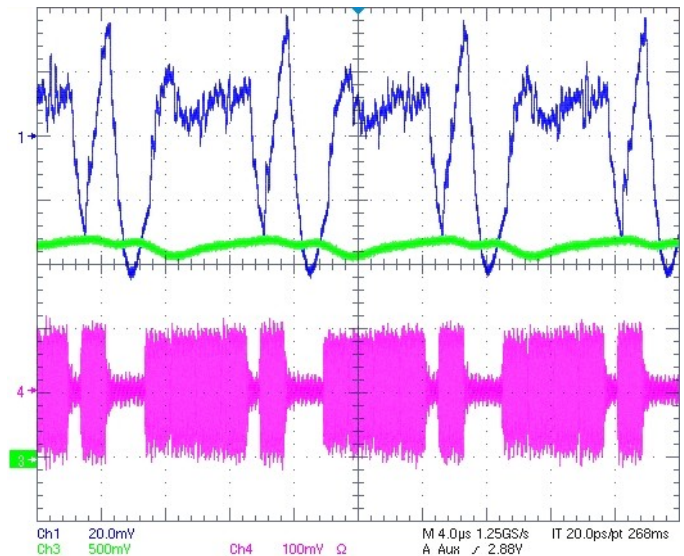


**Figure 3:** SSD forward power monitor 31.6 Vpk into 50 Ohms per module (magenta), modulator output slow current monitor 1A/div (green), modulator output fast current monitor 0.2A/div (blue) on Stal during the 5<sup>th</sup> batch injection of a multi-batch study. Single batch intensity  $\sim 1.7E12$ .

## DC Anode Current During Slipping

In order to confirm the estimate for the RF PA anode DC current of Ref [1], measurements of the Series Tube Modulator (STM) output current were made. Figure 4 shows the STM output current (slow and fast monitors) of station 1 with a single batch of  $\sim 4.4 \text{ E}12$  protons. Station 1 is an 'OFF' station, thus, the tube is attempting to apply equal and opposite compensating current. Due to the overshoot of the fast current monitor and the limited response of the slow current monitor, it is hard to say exactly what the peak instantaneous current is during the batch passing the gap. A worst case estimate can be made if one looks at the baseline to peak excursion of the fast current monitor ( $\sim 4$  amps) and adds that to the minimum of the slow current monitor (3.5 amps). This would imply that the expected current could lie somewhere between 7 to 8 amps. Thus the estimate of Ref [1] ( $\sim 6.5\text{A}$ ) could be in error by 10-20%.

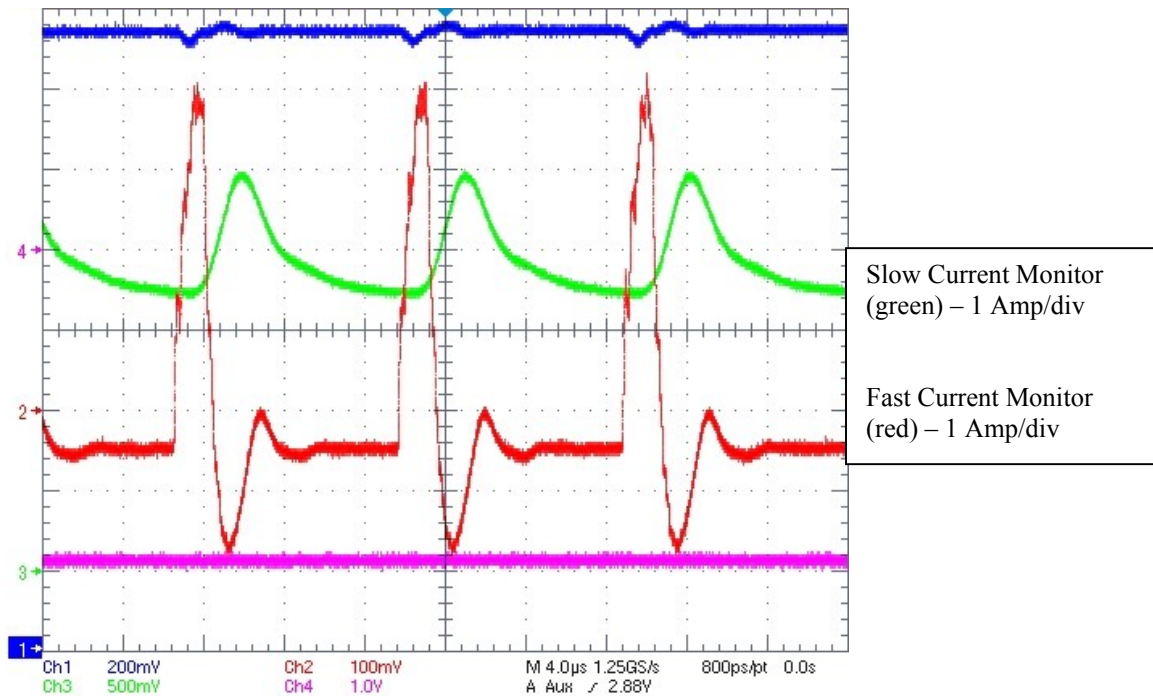


**Figure 4:** Sta 1 (Group A 'OFF' station) Series Tube Modulator fast (red) and slow (green) output current monitors with a single batch of intensity  $\sim 4.4\text{E}12$ .

## Cavity De-Tuning Measurements:

The envelope of the SSD forward power monitor of Fig. 1 is revealing of the present cavity tuning control system. Note that, as more batches are loaded after recapture, the peak instantaneous forward power keeps decreasing. Presently the cavity tuning control system feedback signal is a measurement of the average load angle presented to the RF PA. This signal is derived from a PA anode-to-cathode phase measurement with a band-limited phase detector. There is no tuning offset control. Thus, as more batches are loaded the cavity tuning is adjusted closer to the case of a full ring; whereas at the beginning of a cycle, with the ring only 1/7 full, the cavity is tuned closer to the case of no beam.

To understand the cavity detuning, a software utility (application page W20) was developed. The technique is based upon measuring two parameters; (1) the low-level RF (LLRF) output frequency and (2) the Ferrite Bias Supply (FBS) current. Assuming that the cavity tuning control system is calibrated, the resonant frequency of the cavity is equal to the LLRF output frequency when there is no beam. Thus the cavity resonant frequency can be measured as a function of the FBS current without beam. A 3<sup>rd</sup> order polynomial was found to fit experimental data. Once this function is found without beam, the cavity resonant frequency can be measured by monitoring the FBS current for any condition. This function is not static since the cavities are subjected to temperature changes. Thus it has to be re-measured whenever thermal equilibrium conditions change. An example of the cavity detuning during a mixed-mode cycle is shown in Figs. 5 and 6.

The first two injections are not clearly seen in Figs. 5 and 6 since the cavity tuning of the ‘OFF’ stations are presently ‘held’ before the slip-stacking process begins. The tuning control is ‘released’ at recapture after which the remaining 5 injections are clearly visible. Presently there are also large step-response transients in the tuning control at each injection and step change. The change in the sign of the cavity de-tuning at transition is also clearly visible.

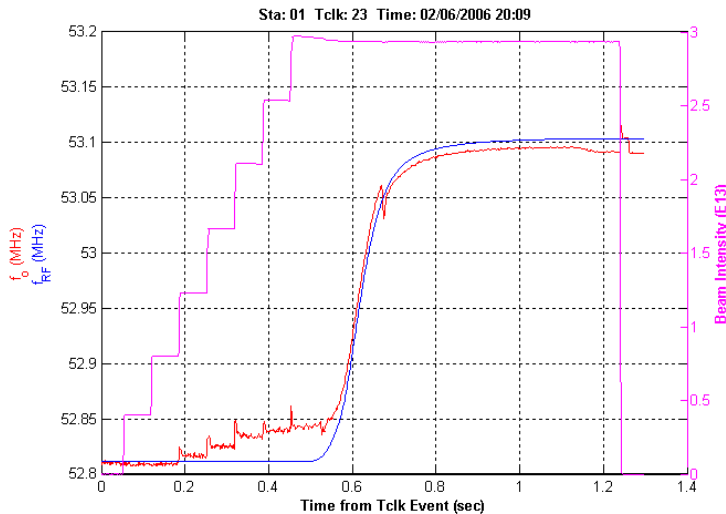


**Figure 5:** Cavity de-tuning measurements during a mixed mode cycle for Station 1 (Group A ‘OFF’ station). Cavity resonant frequency (red), RF drive frequency (blue), beam intensity (magenta).

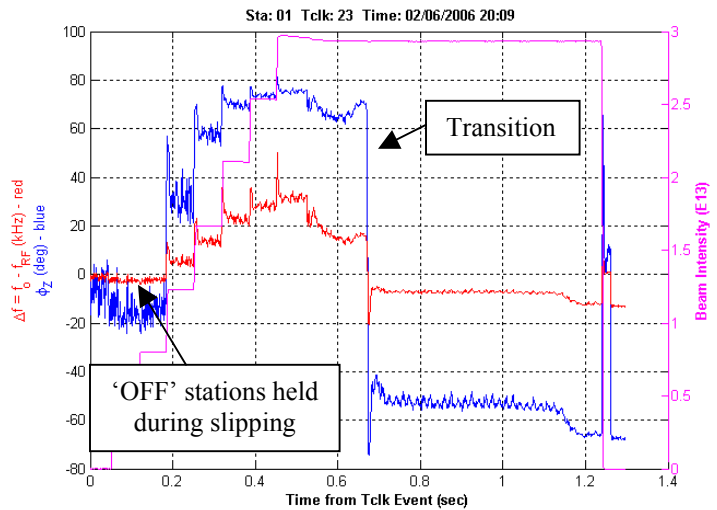


**Figure 6:** Cavity de-tuning measurements during a mixed mode cycle for Station 1.  $\Delta f$  (red), cavity impedance angle (blue), beam intensity (magenta).



To see that the cavity tuning controller is actually determining an ‘average’ load angle, Figs. 7 and 8 show the anode-to-cathode phase detector and SSD forward power on a revolution time scale during the 3<sup>rd</sup> batch and 5<sup>th</sup> batch injection respectively for HLRF station 18 (a Group B ‘ON’ station).

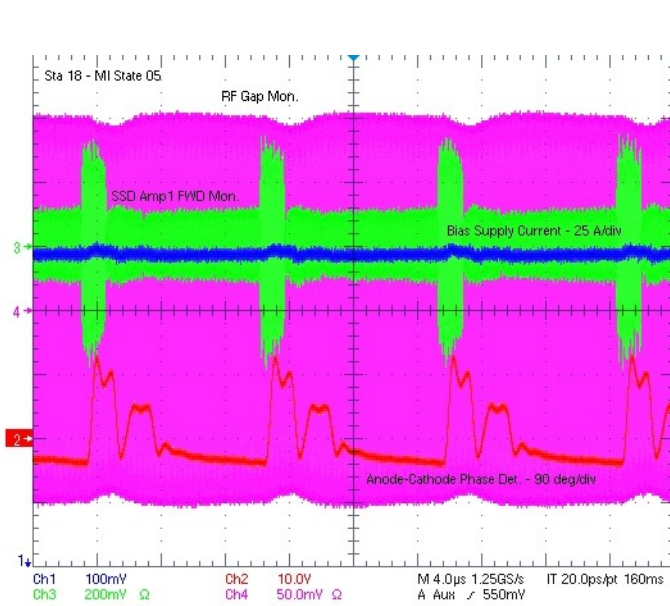


**Figure 7:** Station 18 (Group B ‘ON’ station) cavity detuning control signal immediately after 3<sup>rd</sup> batch injection. Anode-to-Cathode phase detector (red), SSD FWD power monitor (green), RF cavity gap envelope (magenta), FBS current (blue).

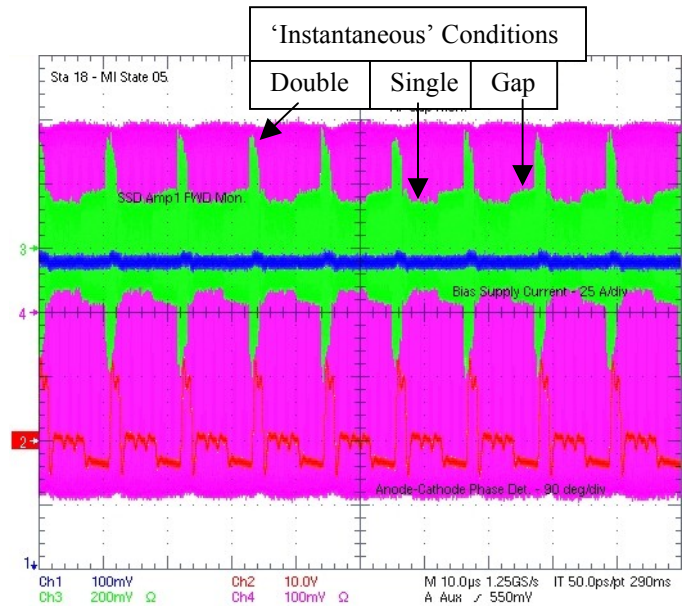


**Figure 8:** Station 18 (Group B ‘ON’ station) cavity detuning control signal immediately after 5<sup>th</sup> batch injection. Anode-to-Cathode phase detector (red), SSD FWD power monitor (green), RF cavity gap envelope (magenta), FBS current (blue).

In both Figs. 7 and 8, the anode-to-cathode phase detector signal averages nearly zero. Unlike an ‘OFF’ station, the FBS current is nearly identical in both cases due to the effect of operating at different gap voltages between the two cases (note the gap monitor scale change); this is a consequence of the pre-MRF system control. Regardless, the overall phase detector signal averages close to zero.

Figures 7 and 8 also justify using the three ‘instantaneous’ conditions in the calculation technique of Ref. [1]. This technique assumed 3 different ‘instantaneous’ conditions within a revolution: (1) a double intensity batch beam current in the cavity, (2) a single intensity batch beam current in the cavity, and (3) a beam gap or no beam current in the cavity. This is clear in Fig. 8 in which there appear to be 3 ‘instantaneous’ SSD forward power levels as notated. Fig. 7 is not as obvious but points to the fact that the cavity tuning controller has settled to a value that is similar to  $\frac{1}{2}$  detuning for a single intensity batch in which the forward power magnitude does not change significantly between the ‘with beam’ and ‘no beam’ conditions.

Another unfortunate consequence of the present cavity tuning control scheme is that the closed loop bandwidth allows the  $\sim 1400$  Hz beat frequency of the two slipping batches to enter into the cavity tuning control. This can be seen in Figs. 9 and 10 which are cavity detuning measurements of a Group A ‘ON’ station and a Group B ‘ON’ station respectively during a multi-batch slip-stacking study.

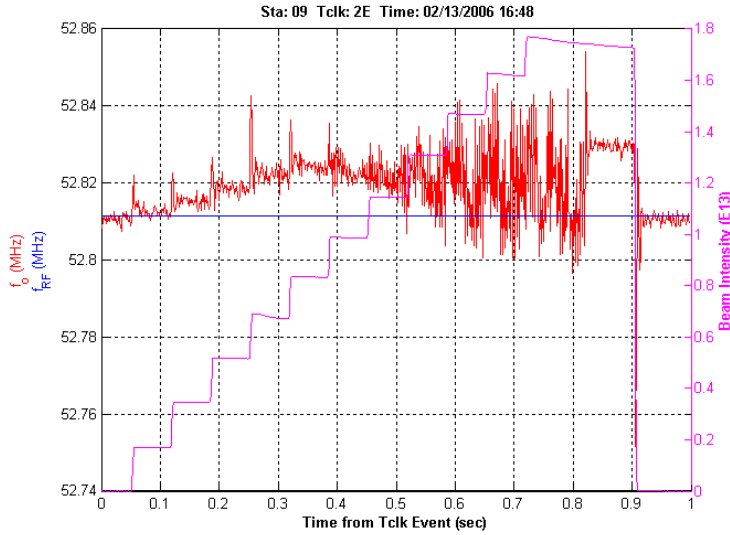


**Figure 9:** Cavity de-tuning measurements during a multi-batch slip-stacking study for Station 9 (Group A ‘ON’ station). Cavity resonant frequency (red), RF drive frequency (blue), beam intensity (magenta).

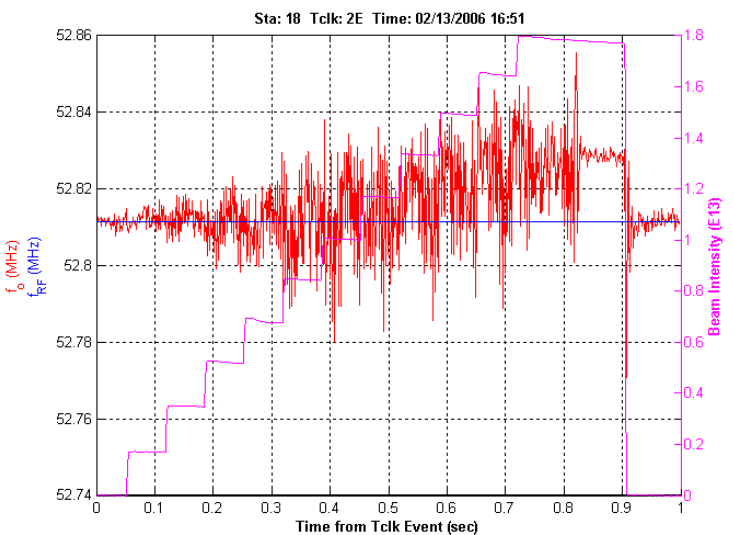


**Figure 10:** Cavity de-tuning measurements during a multi-batch slip-stacking study for Station 18 (Group B ‘ON’ station). Cavity resonant frequency (red), RF drive frequency (blue), beam intensity (magenta).

The cavity resonant frequency modulations are real and are occurring at the beat frequency of  $\sim 1400$ Hz. Note that station 18 begins to see tuning modulations at the 1<sup>st</sup> batch while station 9 doesn’t begin to see the modulations until the 6<sup>th</sup> batch. This is due to the first five batches being injected into the Group A bucket while the last 6 batches are injected into the Group B bucket. The modulations are on the order of  $\pm 10$  to 20 kHz. The tuning modulations can be seen on the FBS current monitor as shown in Figs. 11 and 12 which were taken during a mixed-mode cycle after the 2<sup>nd</sup> batch injection.

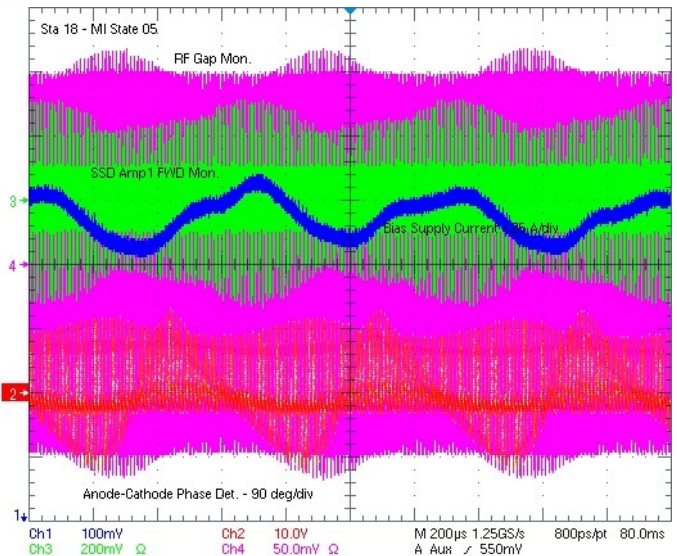
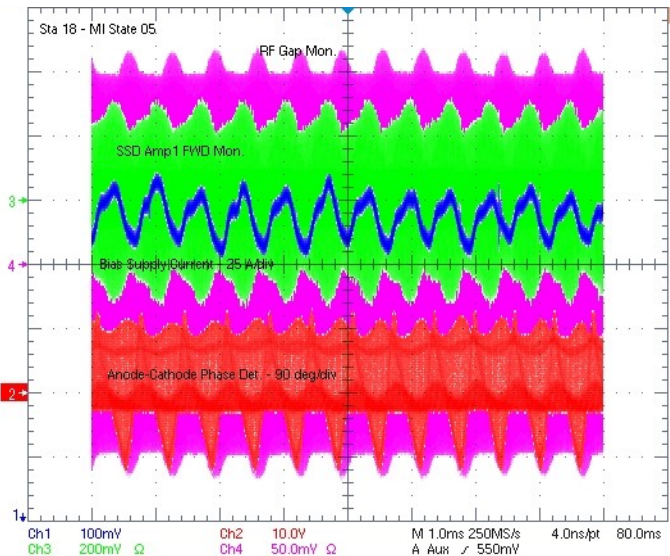


**Figure 11 & 12:** Station 18 (Group B ‘ON’) tuner modulations during a mixed-mode cycle after the 2<sup>nd</sup> batch injection. Zoomed version is on the right. Gap transients are  $\sim \pm 10\%$ . Cavity tuning sensitivity is  $\sim 1$ kHz per FBS amp.

Based upon the above cavity de-tuning measurements, the cavity tuning control scheme could be improved by (1) adding a tuning offset control, (2) improving the transient response of the loop to minimize the large step-response overshoot, and (3) use a fixed tuning during slipping to reduce the tuning modulations induced by the beat frequency of the slipping batches.

### **Summary:**

The measurements confirm that the calculation technique of Ref [1] are valid to first order. Although the measurement of the modulator output current was not straight forward due to the current monitors' dynamic responses, a conservative estimate of the current for the 'OFF' stations reveals that the estimates of Ref [1] may be within 10-20%. A cavity de-tuning measurement utility was developed to quantify the cavity detuning during present operations. Observations of the tuning loop reveal that the tuning control scheme would benefit from the addition of a tuning offset control and improvements to the dynamic response of the loop. The gap transients at flat top could be improved if the FF BLC program was not reduced after transition. Additionally, the SSD forward power requirements appear to be approaching limits of the SSD power supply.

### **References:**

[1] T.Berenc, I.Kourbanis, D.McGinnis, J.Reid, "Main Injector RF Power Requirement Calculations for the Proton Plan", Fermilab beams-doc #2311, June 2006.